

Article

Assessing Efficacy of “Eco-Friendly” and Traditional Copper-Based Antifouling Materials in a Highly Wave-Exposed Environment

Clara Arboleda-Baena ^{1,2} , Nicole Osiadacz ^{1,3}, Mirtala Parragué ^{1,3} , Andrés E. González ¹,
Miriam Fernández ^{1,3,4} , Gerhard R. Finke ^{1,3} and Sergio A. Navarrete ^{1,3,4,5,6,*}

- ¹ Estación Costera de Investigaciones Marinas (ECIM), Las Cruces, Facultad de Ciencias Biológicas, Pontificia Universidad Católica de Chile, Av. Bernardo O'Higgins 340, Santiago 8331150, Chile
 - ² Departamento de Hidrobiología, Universidade Federal de São Carlos, São Carlos 13565-905, Brazil
 - ³ Marine Energy Research and Innovation Center (MERIC), Av. Josemaría Escrivá de Balaguer N° 13105, of. 1011, Santiago 7690000, Chile
 - ⁴ Núcleo Milenio para la Ecología y la Conservación de los Ecosistemas de Arrecifes Mesofóticos Templados (NUTME), Pontificia Universidad Católica de Chile, Santiago 8331150, Chile
 - ⁵ Center for Applied Ecology and Sustainability (CAPES), Pontificia Universidad Católica de Chile, Santiago 8331150, Chile
 - ⁶ Copas Coastal, Universidad de Concepción, Concepción 4070386, Chile
- * Correspondence: snavarrete@bio.puc.cl

Abstract: Biofouling control on human-made structures and seagoing technologies that minimize environmental impacts is a major focus of research in marine industries. However, the most widely used antifouling (AF) method is still copper-based coatings. Some “eco-friendly” approaches are commercially available but have been scarcely tested in natural conditions, especially high-energy environments. We conducted a replicated long-term field experiment in a highly wave-exposed, high productivity coastal environment to test three untreated materials used in maritime industries, two traditional copper-based AF coatings, and two materials offered as “eco-friendly” AF in the market (i.e., a slow-copper release and a self-adhesive, fiber-covered, skin-like coating). We showed that biofouling cover and biomass increased at similar rates over time among all untreated materials, including the skin-like AF. The two traditional copper-based AF coatings and the slow-release AF paint both showed similarly low biofouling biomass and richness, demonstrating their efficacy after 12 months in the field. Although the “eco-friendly” slow-release technologies are not completely innocuous to the environment, we suggest this approach over the more environmentally aggressive traditional copper paints, which are the most widely used in aquaculture and shipping industries today. However, further research is needed to test whether their environmental impact is significantly lower in the long-term than traditional AF paints, and therefore the search for non-toxic coating must continue. The fortuitous settlement and growth of sea urchins in our experiments also suggest that a combination of “eco-friendly” AF and biological control would be possible and should be further investigated. The skin-like coatings must be tested under different environmental conditions, and they are not recommended in wave-exposed coastal habitats.

Keywords: marine biofouling; replicated field experiments; subtidal habitats; grazing and biological control; upwelling ecosystems; tunicates; barnacles



Citation: Arboleda-Baena, C.; Osiadacz, N.; Parragué, M.; González, A.E.; Fernández, M.; Finke, G.R.; Navarrete, S.A. Assessing Efficacy of “Eco-Friendly” and Traditional Copper-Based Antifouling Materials in a Highly Wave-Exposed Environment. *J. Mar. Sci. Eng.* **2023**, *11*, 217. <https://doi.org/10.3390/jmse11010217>

Academic Editor: Francesca Cima

Received: 12 December 2022

Revised: 29 December 2022

Accepted: 30 December 2022

Published: 13 January 2023



Copyright: © 2023 by the authors. Licensee MDPI, Basel, Switzerland. This article is an open access article distributed under the terms and conditions of the Creative Commons Attribution (CC BY) license (<https://creativecommons.org/licenses/by/4.0/>).

1. Introduction

Marine biofouling is the community of organisms that establishes, grows, and accumulates on natural or artificial surfaces immersed in sea water. Biofouling growth begins with the rapid formation of microbial biofilms on substrates, followed by settlement of macroinvertebrate larvae and macroalgal spores, which grow, gain biomass, and overgrow the original biofilm [1,2]. As the succession progresses over months and years, the composition

of species changes and larger body size species which usually are competitively dominant in the interference for space [3,4] tend to dominate the substrate [5]. Problems caused by biofouling—such as increased corrosion, higher biomass (weight), increased drag forces, introduction of invasive species, lower flow, and deoxygenation—are commonly reported by the aquaculture and shipping industries [6,7] due to the incredibly detrimental economic impacts they have in those industries [8]. The emerging marine renewable energy industry (MRE) and the development of mechanical energy converters are especially afflicted by biofouling [9]. To counter these difficulties, different biofouling control strategies have been proposed: chemical, mechanical, biological, electrochemical, and surface modification [10]. The chemical control known as coating is currently the most common antifouling (AF) strategy, is designed to be effective against various taxa and environmental conditions and has comparatively long durability. These AF coatings are based on an active principle and a matrix. The former consists of one or more toxic biocides that target the early stages of the fouling species (since adult organisms are usually more resistant to these products) while the matrix has the binders, solvents, and auxiliary compounds that provide support, adhesion, and durability to the active components [11]. The most widespread active principles are copper oxide (Cu_2O), Cu(I) thiocyanate, and Zn(II) oxide [12], while the developed matrices include the soluble, contact leaching, self-polishing copolymer (SPC) and fouling-release matrix coatings [6]. Since all toxic chemical AF strategies come at a cost for the environment, there is broad interest in eco-friendly strategies that do not pollute as much [6,13,14].

The release of high concentrations of these biocide compounds into the environment poses a danger to marine organisms [14–17]. It is estimated that over 15×10^6 kg/year of copper is introduced to the ocean environment by AF paints worldwide [18]. Consequently, research focuses on developing coatings that either release fewer compounds into the environment, physically modify the surface without chemically active components, or incorporate active components that are produced by local organisms [13,19]. However, the use of natural broad-spectrum antifoulants is still far from commercialization [5,19]. Copper oxide nanoparticles are both marketed for use in antifouling paints as an “eco-friendly” alternative and found in commercially available coatings [20]. Based primarily on laboratory studies, the manufacturers insist that nanoparticles can be retained in the paint matrix, reducing leaching and increasing the timespan of AF efficacy. However, their efficacy and durability under natural (field) conditions and diverse forms of biofouling have scarcely been tested. Nanoparticle paints with ZnO are also now available; similar to other zinc-based coatings, they are marketed as “eco-friendly” alternatives [21]. Caution must be exercised in real applications, however, as recent research suggests that there is no clear advantage of nanoparticulate Zn or Cu in antifouling coatings, relative to traditional micro-sized formulations, either in their efficacy or toxin release characteristics [21]. Another strategy for reducing Cu_2O leaching is the controlled depletion polymer (CDP), which has a controlled and stable release over time and increases the AF efficacy lifespan [22].

Ecological control of biofouling is also possible for some specific applications. Here, species interactions keep the most harmful fouling species in check, usually reverting ecological succession to initial stages. Several studies considering fouling on marine structures have shown the potential of biological control alone [23] and in combination with other AF methods [24]. For example, grazing (apparently due to sea urchins) reduces biofouling cover and biomass on artificial structures [23,25,26]. Grazers can also reduce biofouling growth within shellfish aquaculture farms [26–28] and may provide control for invasive algae [29,30]. Thus, biological control, combined with other AF methods, seems promising for some applications [31].

Most knowledge about biofouling and most experimental tests of AF methods have been conducted in the laboratory or in wave-protected habitats, usually within bays and port harbors. The requirements of the MRE, oceanic aquaculture, desalination, and other industries are rapidly expanding this knowledge to high-energy environments [32–35]. We conducted a replicated field experiment over more than one year in a highly wave-exposed

environment to test biofouling colonization and accumulation rates on three different materials typically used in the shipping, aquaculture, and desalination industries. In addition, we tested two traditional (non-ecofriendly) copper-based AF coatings that are the most widely used in the industry, and two AF strategies labeled “eco-friendly” (a skin-like coating that modifies substrate surface and a copper slow-release AF paint). The experiment was followed for 15 months at two different depths to assess both changes in the relative performances of these varied strategies and the performance of the different materials and AF strategies over the ecological succession towards dominant sessile species [33]. Through the course of the field experiment, an unexpected and massive recruitment of the black omnivorous sea urchin *Tetrapygus niger* occurred, allowing us to obtain a preliminary assessment of the potential for sea urchin grazing as a biological control for biofouling biomass.

2. Materials and Methods

2.1. Study Site, Environmental Variables

The study was conducted in the Bay of Cartagena, a section of the central Chilean coast that is fully exposed to the predominant incoming waves propagating from the south (<http://www.oleaje.uv.cl/pronostico.htm>, accessed on 29 December 2022) (Figure 1). While the Chilean shore is characterized by a strong coastal upwelling of subsurface, cold, nutrient-rich waters, the Bay of Cartagena is in an upwelling shadow, with slightly warmer waters (1–2 °C), slightly fewer nutrients, and more frequent phytoplankton blooms than at sites to the north and south [36–38]. The general hydrographic characteristics of the study site—including broad patterns of circulation related to wind forcing, phytoplankton, wave regimes, and riverine inputs—have been previously described [36,39–44]. In addition, the encrusting community of wave-exposed environments and successional trends at different depths have been previously described [32,33].

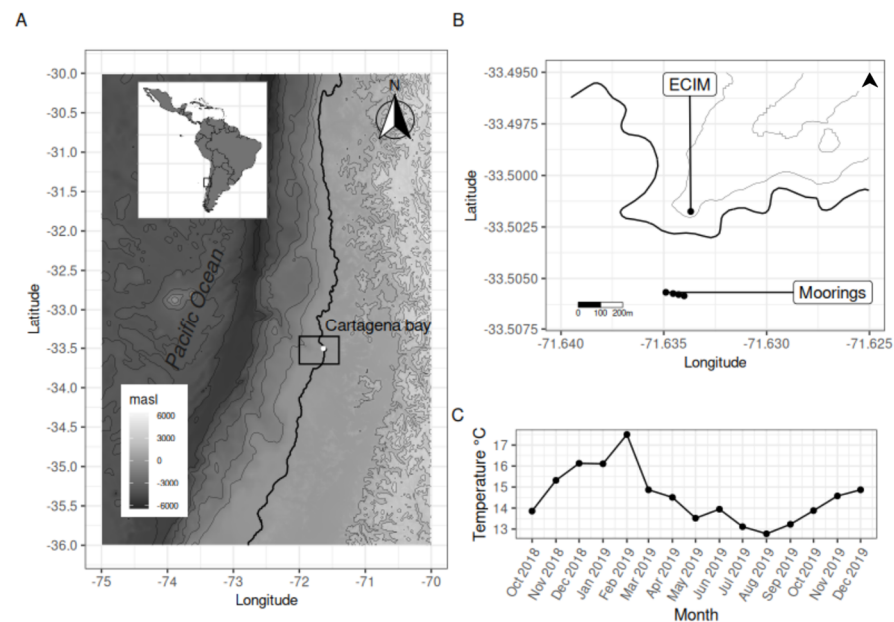


Figure 1. (A) Map of study site at Bay of Cartagena in central Chile. (B) Position of the four moorings (the plates are facing the compass direction). (C) Seawater average temperature at 5 m deep between October 2018 and December 2019.

2.2. Mooring, Testing Frames, and Monitoring Schedule

In October 2018, we deployed four moorings at 20–21 m bottom depths spread over ca. 80 m and separated by ca. 20 m (Figure 1 and Supplementary Materials Figure S1). Each mooring consisted of a 150 kg weight and a high-tenacity Dynema rope. A subsurface buoy at about 1 m deep at the end of the line, and two small (50 cm diameter) buoys along the

rope were used to keep the line taut, even during passing waves. Testing frames were made of 2.5 cm diameter hydraulic-rated polyvinyl chloride (PVC), forming a 70 × 40 cm rectangle [32]. At each mooring, two testing frames were deployed, one at 5 m deep, above the seasonal thermocline [36,39], and the other one at ca. 15 m deep, below the thermocline (Supplementary Materials Figure S1). Temperature loggers (Onset Tidbit®) were attached to one mooring line, which recorded the temperature every 10 min at ca. 2 m depth, above the first frame, and at ca. 19 m depth, below the deeper frame.

2.3. Materials and Antifouling Treatments

Experimental treatments were applied to 10 × 10 cm plates that were attached with stainless steel bolts to the PVC testing frames at each depth. A total of seven treatments were deployed randomly in testing frames at each depth and four moorings. First, three different traditional and untreated materials were tested. The first was 4–6 cm thick acrylic plates (Plexiglass®) that were evenly roughened by sanding the plate surface. This material has been widely used in previous studies of encrusting organisms in Chile [32,33,45–47] and serves as a reference for biofouling settling. The second was a steel (Steel A32) construction plate used in the shipping industry and MER converters, and the third was a stainless steel (Steel 304) construction plate used in several seagoing applications. The Steel A32 plates rusted within few months, causing the metal to laminate and peel off the plate with organisms attached. As a result, these plates were not included in the analyses described below, leaving only two untreated materials to be compared. Second, we compared two market-available AF strategies labeled “eco-friendly”. The first was a modified substrate surface coating known as Micanti. This is a nylon fiber and polyester film with a furry texture and a two-component water-based adhesive marketed as an “eco-friendly” “hairy” solution to fouling, primarily for the shipping industry. It is advertised as suitable for all circumstances (i.e., moored or sailing). The second is Seavoyage 100 CDP Sherwin-Williams (CDP), a copper-based, slow-release (controlled wear polymer), AF paint marketed as “eco-friendly”. Like all copper-based paints, it can pollute the environment in the mid- to long-term but has gained the “eco-friendly” label, so we refer to it as such. The third and fourth materials we considered were two widely available copper-based AF paints that have not been designated eco-friendly, Seavoyage A/F-21 Sherwin-Williams (F21) and Ocean Jet 33 (OJ33). Treatment chemical characteristics, applications, and manufacturer descriptions are presented in Supplementary Materials Table S1. Steel plates (A36) with AF were painted in San Antonio, Chile, following the same procedures used in ships. The steel surface roughness (RMS) was 6.6 μm [32].

2.4. Successional Treatments and Monitoring Protocol

To test for differences in ecological succession in the above treatments, we performed three exposure time treatments: (a) exposure in the field for 6 months, during the first phase of the experiment (first six months (First6): October 2018–April 2019), (b) exposure in the field for approximately 6 months during the second phase of the experiment (second six months (Second6): April 2019–January 2020), and (c) exposure for 15 continuous months (yearly: October 2018–January 2020). This allowed us to assess temporal differences among materials and antifouling treatments during short- and long-term exposure. Thus, at each experimental frame, depth, and mooring, 14 plates were deployed; 7 of them were removed after 6 months and replaced with new ones, and the other 7 were monitored while submerged throughout the experiment. The size and the hydraulic behavior of the frame did not allow us to include replication within the frames, so plates across the four moorings were considered replicates. This is consistent with a randomized complete block design with material treatments and successional times (see below) applied to one replicate plate within each block [48].

Before deployment, each plate was weighed on a scale, both dry and submerged in water, and then individually marked with a serial number. To monitor the experiment, plates were photographed in situ by SCUBA divers every 3 months. Every 3–4 months, we

removed the plates from their frames, aboard the research boat of the Estación Costera de Investigaciones Marinas (ECIM), we carefully cleaned the sides and weighed each plate. Then, we recorded species cover with a 10×10 -cm quadrat with 100 intersection points.

We removed each plate after its predetermined immersion times (ca. 6 or 15 months) and taken to the Biocorrosion and Biofouling Laboratory at ECIM. There, we drained the plates for 1 min and weighed them. We obtained the total biofouling mass by subtracting the plate's initial mass. We then identified and quantified the main encrusting species under a stereo microscope using the same protocol as used on the boat (i.e., 10×10 cm quadrat with 100 intersection points). We then photographed the tops and sides of each plate (see Supplementary Materials Table S2).

2.5. Data Analyses

During the experiment, we observed a massive settlement and growth of the black sea urchin *Tetrapygus niger* on all plates, especially at shallower depths (see results below). Settlement of *T. niger* was unusually high in the 2019 recruitment season (see Supplementary Materials Figure S2). The small settlers were apparent by December 2018, roughly 60 days after the experiment had been deployed. Since this was a natural occurrence (although it had not been seen the previous 3 years at the same site [33]), we did not remove the sea urchins in order to leave other settlers undisturbed. We continued monitoring the experiment until September 2019, so our results reflect community succession under the grazing pressure of sea urchins. To assess the impact of urchins on sessile organisms, in September 2019 (317 days after the experiment began), we carefully removed all urchin recruits and juveniles from both the plates and frames, and then continued to monitor the experiment again in January 2020. Thus, we conducted the analyses described below separately. The two distinct periods—before manual urchin removal and after—may be considered as observations of sessile species patterns with grazing pressure and without grazing pressure, respectively.

2.6. Biofouling Biomass

Because the time between monitoring events varied due to sea conditions, we divided each plate's total biofouling mass by days elapsed, thus obtaining a rate of mass accumulation expressed as grams per day in 100 cm^2 [33]. As shown before, total biofouling weight is a better indicator of biofouling risks than surface cover, since in these environments, sessile species quickly cover entire substrata, despite major compositional changes through succession [33]. Before analyses, we averaged each replicate plate's multiple weight observations obtained during on-board measurements, simplifying analyses and eliminating the need for repeated measures. We performed separate analyses for the period before sea urchin recruits and juveniles were manually removed (first 317 days) and for the observations collected 139 days after removal.

We performed a three-way factorial analysis of variance (ANOVA) on mean biofouling biomass accumulation ($\text{g/day}/100 \text{ cm}^2 \pm \text{SE}$), considering the traditional materials and AF treatments (Steel A32 was dropped from analyses), the three successional treatments (First6, Second6, and Yearly), and the two depths as fixed orthogonal factors, applied within each block (testing frame). We performed separate a priori orthogonal contrasts [49] at 5 and 15 m deep to test the specific hypotheses about main effects stated in Table 1. In case of interactions, we used the corresponding orthogonal contrasts for the interaction (see [50]). Before analyses, biomass data were logit-transformed for the first 6 months to satisfy the ANOVA's homoscedasticity assumptions.

Table 1. Specific hypotheses and planned orthogonal contrasts for main effects treatments at each depth.

Treatment	Main Effects Hypotheses	Planned Contrasts
Exposure time	Biomass accumulation means are different between early and late succession	First6 and Second6 <i>versus</i> Yearly
	Biomass accumulation means are different between the first and second parts of the experiment	First6 <i>versus</i> Second6
Traditional maritime industry materials and AF coatings	Traditional materials are different from copper-based, not eco-friendly, AF coatings	Acrylic and SS316 <i>versus</i> OJ33 and F21
“Eco-friendly” strategies and copper-based, not eco-friendly, AF coatings	“Eco-friendly” strategies are different from copper-based, not eco-friendly AF coatings	Micanti and CDP <i>versus</i> OJ33 and F21
“Eco-friendly” AF strategies	The two “eco-friendly” strategies are different	Micanti <i>versus</i> CDP

To examine whether the response to urchin removal was similar among treatments and depths, we calculated the biofouling biomass accumulation rate (g/day/100 cm² ± SE) for the observations collected in January 2020, after urchin removal, and analyzed results with a two-way ANOVA randomized block design with materials and AF treatments (acrylic, stainless steel, Micanti, CDP, F21, and OJ33) and depths (5 and 15 m) as fixed factors, and mooring as block. Biomass accumulation rate was square root transformed to obtain normality and homoscedasticity. One mooring line was lost due to storms, so we conducted the analysis using 3 mooring replicates. We performed a Tukey post-hoc test. In this case, the results refer to effects on recovery of the biofouling community after removing grazers.

2.7. Biofouling Cover

We calculated mean total biofouling cover per plate (%) with all species pooled, (excluding biofilms) for all monitoring dates with complete datasets for the yearly successional exposure treatment. The design included only the material and antifouling treatment and the two depths as fixed factors, but with multiple repeated observations on each plate for the period before sea urchin removal. We analyzed these data with a repeated measures analysis of variance (RM-ANOVA) after checking for sphericity with the Mauchly criteria. We did not analyze total cover in the two 6-month exposure treatments. A simple two-way ANOVA with material and AF treatment and depth was used to analyze total cover after sea urchin removal.

The cover of the dominant three sessile species—*Austromegabalanus psittacus* (Molina, 1782), *Obelia geniculata* (Linnaeus, 1758), and *Pyura chilensis* (Molina, 1782)—accounted for 22–100% of the total cover. These analyses, conducted as described above for total cover, considered only the acrylic, stainless steel, and Micanti treatments because the species were found at very low cover in the other treatments (see Section 3). We constructed all graphics and performed all statistical analyses in R [51,52].

2.8. Biofouling Community Analyses

To characterize community compositional differences and general structure among material treatments and exposure months, we conducted multivariate ordinations on species abundances (cover) using the Bray Curtis distance method and non-metric multidimensional scaling. To test for statistical significance, we conducted a permutational analysis of variance (PERMANOVA) [53] followed by pairwise a posteriori tests using the false

discovery rate (FDR) correction [54]. For the multivariate analyses, we used the R package *vegan* v2.5-7 [55]. After ensuring normality and homoscedasticity, we conducted separate one-way analyses of variance on richness and the Shannon diversity index to compare richness and diversity among treatments. We considered treatment and depth as fixed factors and used Dunn’s post-hoc test to establish the pattern of differences.

3. Results

The main species of biofouling communities at different treatment were biofilm, *Obelia geniculata*, *Austromegabalanus psittacus*, and *Pyura chilensis*. We included the complete list of species and their maximum cover percentage throughout the experiment in Supplementary Materials Table S3. We removed the steel treatment for all analyses due to the high percentage of surface oxide (Supplementary Materials Table S3), which accelerated the corrosion process, although we had periodically removed biofouling biomass along with corroded metal (see Supplementary Materials Figure S3). The corrosion and biomass loss in Steel A32 treatment can be explained by the deterioration of the coating that favors the alteration of the electrical conductivity of materials [56].

3.1. Biofouling Biomass

During natural succession, the mean biomass accumulation rates (g/day/100 cm²) (Figure 2) at 5 m were higher on acrylic, stainless steel, and Micanti plates after ~120 days and higher on the same treatment plates at 15 m deep after ~180 days. After ~365 days of deployment, sea urchins were removed from all plates at both depths. The mean biofouling biomass accumulation rates on the acrylic, stainless steel, and Micanti treatments all increased significantly at 5 m (Figure 2).

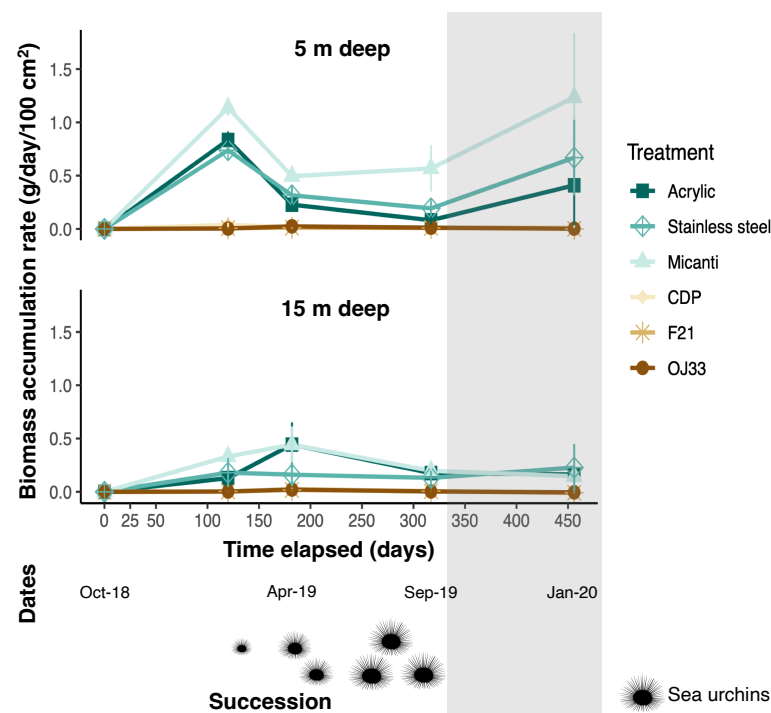


Figure 2. Biofouling biomass accumulation rate (g/day/cm² ± SE) in the 100 cm² plates recorded during 15 months at the two depths of deployment. Plates were replaced. The bottom scheme shows when sea urchin recruits were first observed in the experimental moorings, and when they grew and increased in abundance on the plates. The shading shows biomass trajectories after sea urchin manual removal on day 317 of the experiment.

For the plates exposed for 12 months (before sea urchin removal), we found significant differences in the mean biofouling biomass accumulation (g/day/100 cm² ± SE) in exposure

time ($p < 0.001$), treatments ($p < 0.001$), depths ($p < 0.001$) and the interaction between exposure time and treatments ($p < 0.001$) (see Figure 3 and Supplementary Materials Table S4.1). However, we did not find differences between the interaction exposure time–depth ($p = 0.641$), treatment–depth ($p = 0.331$), and exposure time–treatment–depth ($p = 0.171$) (see Supplementary Materials Table S4.1).

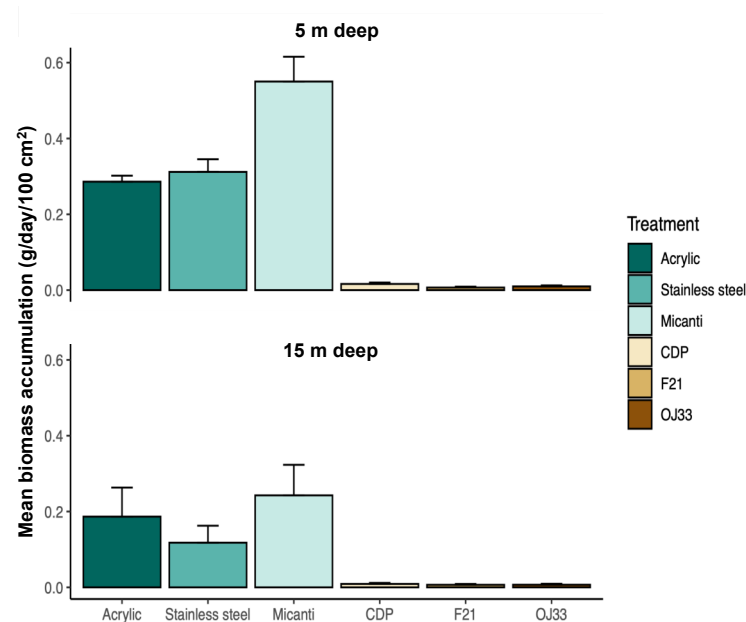


Figure 3. Mean biomass accumulation (g/day/100 cm² ± SE) in the different experimental materials and coatings over 12 months of exposure at the two depths of deployment, before urchin removal.

Likewise, we found significant differences in mean biomass accumulation (g/day/100 cm² ± SE) in some of the linear a priori contrasts analyzed (Table 1 and Figure 4). In the exposure time treatment, the mean biomass accumulation was different during early versus late succession (planned contrast First6 and Second6 versus Yearly, $p < 0.001$). The mean biomass accumulation was also different between the first and second 6-month periods (planned contrast First6 versus Second6, $p < 0.001$). For treatments, materials without AF coatings were different to materials with copper-based, not eco-friendly, AF coatings (planned contrast untreated materials acrylic and SS316 versus treated materials OJ33 and F21, $p < 0.001$). “Eco-friendly” AF coatings also were different to copper-based, not eco-friendly, AF coatings (planned contrast OJ33 and F21 versus Micanti and CDP, $p < 0.001$). Finally, the two “eco-friendly” coatings were significantly different (planned contrast Micanti versus CDP, $p < 0.001$). The copper-based, not eco-friendly, AF coatings were not significantly different from one another (planned contrast F21 and OJ33, $p = 0.91$) (see Figure 4 and Supplementary Materials Table S4.1).

The interaction between exposure time and treatments showed that difference between the mean biomass accumulation of treated and untreated materials can be explained by the exposure time ($p = 0.022$). However, exposure time cannot explain the differences in mean biomass accumulation between copper-based, not eco-friendly, AF coatings (F21 and OJ33) versus “eco-friendly”, AF coatings (Micanti and CDP; $p = 0.746$). Similarly, exposure time also does not explain the differences of mean biomass accumulation between the “eco-friendly”, AF coatings (Micanti and CDP, $p = 0.717$) and the copper-based, not eco-friendly, AF coatings (F21 and OJ33, $p = 0.659$).

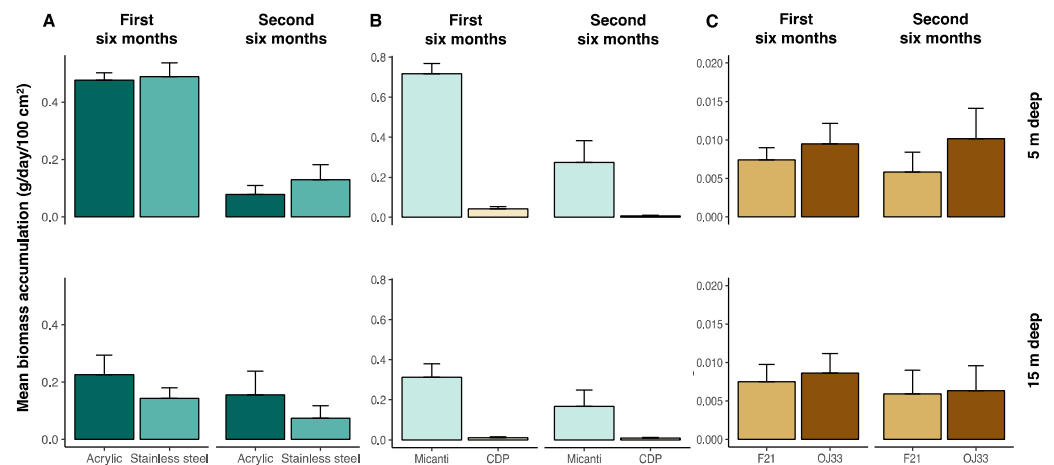


Figure 4. Mean biomass accumulation ($\text{g/day}/100 \text{ cm}^2 \pm \text{SE}$) on each plate, deployed at different times during the first and second 6 months of the experiment at the two deployment depths. (A) Untreated materials (acrylic versus stainless steel), (B) the two “eco-friendly” AF strategies (Micanti versus CDP), and (C) the two not eco-friendly AF paintings (F21 versus OJ33). Note the different y -axis scales.

We found that mean biomass accumulation differed significantly between treated (F21 and OJ33) and untreated materials (acrylic and stainless steel), as well as between copper-based, not eco-friendly, AF coatings (F21 and OJ33) and “eco-friendly” AF coatings (CDP and Micanti). These differences are explained by the two experiment periods (i.e., first and second 6 months exposure, $p < 0.0001$ and $p = 0.005$, respectively). However, these two periods do not explain the differences in mean biomass accumulation between the “eco-friendly”, AF paintings (CDP versus Micanti, $p = 0.077$) nor between the copper-based, not eco-friendly, AF coatings (F21 versus OJ33, $p = 0.976$) (see Figure 4 and Supplementary Materials Table S4.1).

The randomized block designs we performed to analyze the indirect effect of urchin removal on the mean biofouling biomass accumulation showed significant differences between treatment ($p = 0.0005$) and depth ($p = 0.012$), but not mooring ($p = 0.583$) nor the treatment–depth interaction ($p = 0.306$) (Supplementary Materials Table S4.2). Although the interaction was not significant, it should be noted that, after urchin removal, Micanti at 5 m deep differed from the CDP, F21, and OJ33 treatments at 5 and 15 m deep. The treatments that varied the most after urchin removal were Micanti versus CDP, F21, and OJ33 (Supplementary Materials Table S4.2, Tukey post-hoc test, $p < 0.008$) and stainless steel versus F21 (Supplementary Materials Table S4.2, Tukey post-hoc test, $p = 0.042$).

3.2. Biofouling Cover and Dominant Species

The acrylic, stainless steel, and Micanti treatments reached maximum cover percentage of ~100% at 5 and 15 m deep before and after urchin removal (12 and 15 months, respectively) (Figure 5). After 15 months, the mean cover percentage of sessile species during the natural succession (12 months) on the AF painting plates at 5 m was less than 15% (CDP), 8% (F21), and 19% (OJ33), while at 15 m, mean coverage was less than 4% (CDP), 6% (F21), and 3% (OJ33). After the urchin removal, the treatments reached a mean cover percentage of 33% (CDP), 11% (F21), and 12% (OJ33) at 5 m, and 12% (CDP), 8% (F21), and 13% (OJ33) at 15 m (Figure 5).

We did not find significant differences in biofouling mean cover percentage of sessile species at 12 months between acrylic, stainless steel, and Micanti treatments at 5 and 15 m (RM-ANOVA, $p = 0.09$; Supplementary Materials Table S5). Furthermore, after the urchin removal, we did not find significant differences between these treatments at either depth (ANOVA, $p > 0.07$, Supplementary Materials Table S5).

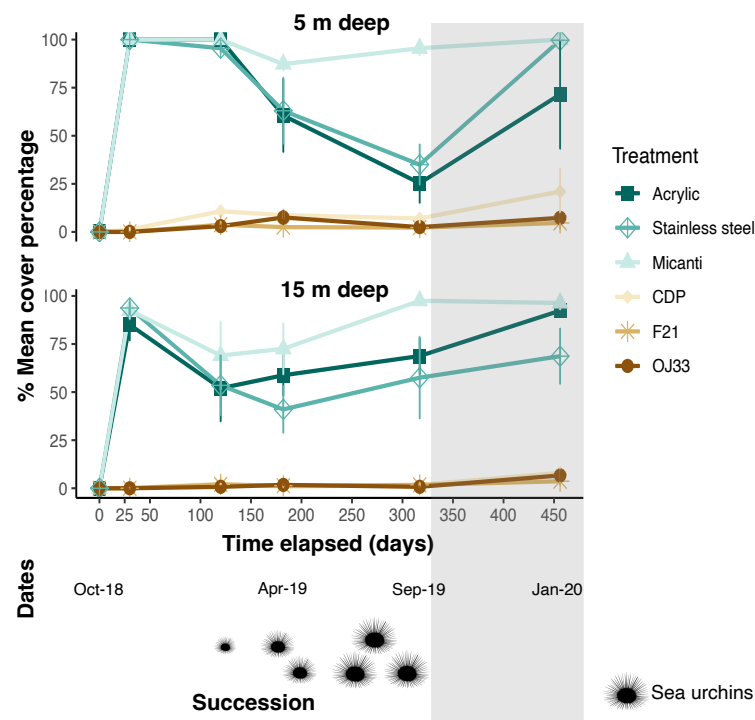


Figure 5. Mean cover percentage (% ± SE) in the 100 cm² plates recorded during 15 months at the two depths of deployment. Biofilms cover data was removed. The shade represents biomass accumulation rates post-sea urchin removal.

The main sessile biofouling species we encountered were *Austromegabalanus psittacus*, *Obelia geniculata*, and *Pyura chilensis*. After 15 months at 5 m, the mean coverage of *Obelia geniculata* was high (>98%) for the first months on stainless steel and Micanti, and *Pyura chilensis* also showed a gain in coverage in the same treatments (56.3% and 91%, respectively) (Figure 6A). *Obelia geniculata* showed the same pattern on acrylic plates (96%) in the first months, but after the sixth month, both *Austromegabalanus psittacus* (36.5%) and *Pyura chilensis* (7.3%) increased their average coverage. The CDP, F21, and OJ33 treatments showed the lowest average cover percentage of these three species throughout the entire experiment at this depth. At the end of the experiment, *Obelia geniculata* and *Austromegabalanus psittacus* showed an average coverage of 11% and 6.5% in CDP, 2.3% and 1.3% in F21a, and 6% and 1.7% in OJ33, respectively. *Pyura chilensis* did not appear on the CDP, F21, and OJ33 treatment plates throughout the 15 months of exposure.

At 15 m, *Obelia geniculata* showed higher mean coverage (>85%) for 4 months, when *Austromegabalanus psittacus* increased its coverage on acrylic (37%) and stainless steel (41%) plates; *Obelia geniculata* showed higher coverage (92%) for 6 months on Micanti, when *Pyura chilensis* gained coverage (33%) at the end of the experiment (Figure 6B). At 15 m deep, CDP, F21, and OJ33 treatments showed a low average coverage of these species throughout the experiment (i.e., less than 5%).

In summary, at 5 m, the mean coverage of *Austromegabalanus psittacus* is most affected by depth, *Obelia geniculata* is most affected by treatment (although Micanti does not have an AF effect), and *Pyura chilensis* favors Micanti.

The main biofouling species in CDP, F21, and OJ33 treatments were biofilm, *Obelia geniculata*, *Antithamnion densum* (M. Howe, 1914), and *Austromegabalanus psittacus* (Molina, 1788). On CDP treatment plates, *Aulacomya ater* (Molina, 1782), *Heterosiphonia* spp., and *Sycon* spp. also recruited. F21 hosted *Heterosiphonia* spp. and *Semimytilus algosus* (Gould, 1850), and OJ33 had *Aulacomya ater* and a member of the family Kallymeniaceae.

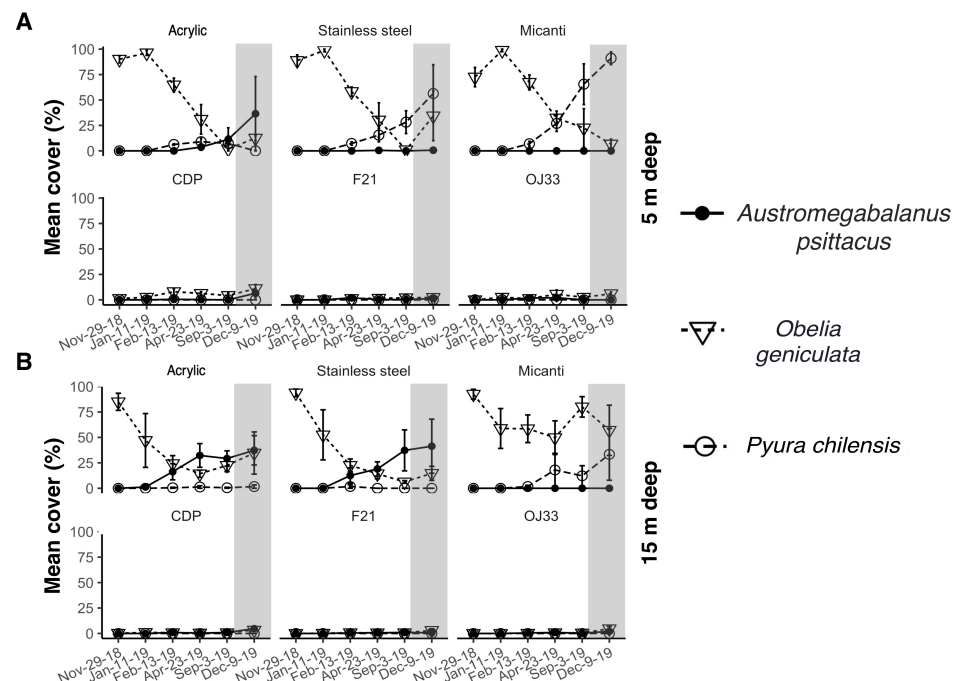


Figure 6. Mean cover (% ± SE) of the most abundant sessile biofouling species, *Austromegabalanus psittacus*, *Obelia geniculata*, and *Pyura chilensis*, observed on acrylic, stainless steel, Micanti, CDP, F21 and OJ33 plates, during 15 months at the two depths of deployment (A) 5 m and (B) 15 m. Gray shadow shows trajectories post-sea urchin removal.

3.3. Biofouling Community

Differences in the similarity of biofouling communities after 12 months of exposure were significant at 5 m (PERMANOVA, $df = 5$, $p = 0.001$, Figure 7A), and 15 m (PERMANOVA, $df = 5$, $p = 0.001$, Figure 7B). At 5 m, we observed two groups with similar composition: group 1 (acrylic, stainless steel, and Micanti) (FDR post-hoc tests, adjusted $p > 0.8$) and group 2 (CDP, F21, and OJ33) (FDR post-hoc tests, adjusted $p > 0.5$). Both groups showed significant differences between them (FDR post-hoc tests, adjusted $p = 0.015$) (see Supplementary Materials Table S5). At 15 m, we observed three groups: group 3 (acrylic and stainless steel), group 4 (Micanti), and group 2 (CDP, F21, and OJ33) (FDR post-hoc tests, adjusted $p = 1.0$). All groups showed statistical differences between them (FDR post-hoc tests, adjusted $p = 0.015$) (see Supplementary Materials Table S5).

After the first 6 months of exposure, differences in the similarity of biofouling communities were significant at 5 m (PERMANOVA, $df = 5$, $p = 0.001$, Figure 7C) and two groups were observed: group 1 (FDR post-hoc tests, adjusted $p = 1$) and group 2 (FDR post-hoc tests, adjusted $p = 1$) (Supplementary Materials Table S5). We also found significant differences in the similarity of biofouling communities at 15 m (PERMANOVA, $df = 5$, $p = 0.001$, Figure 7D). Micanti differed from all other treatments (FDR post-hoc tests, adjusted $p < 0.04$), while CDP, F21, and OJ33 were similar to each other (FDR post-hoc tests, adjusted $p > 0.96$).

After the second 6 months of exposure, the similarity of biofouling communities were significant at 5 and 15 m (PERMANOVA, $df = 5$, $p = 0.001$, Figure 7E,F), but it was not possible to discriminate which groups that differed from each other based on FDR post-hoc tests (see Supplementary Materials Table S5).

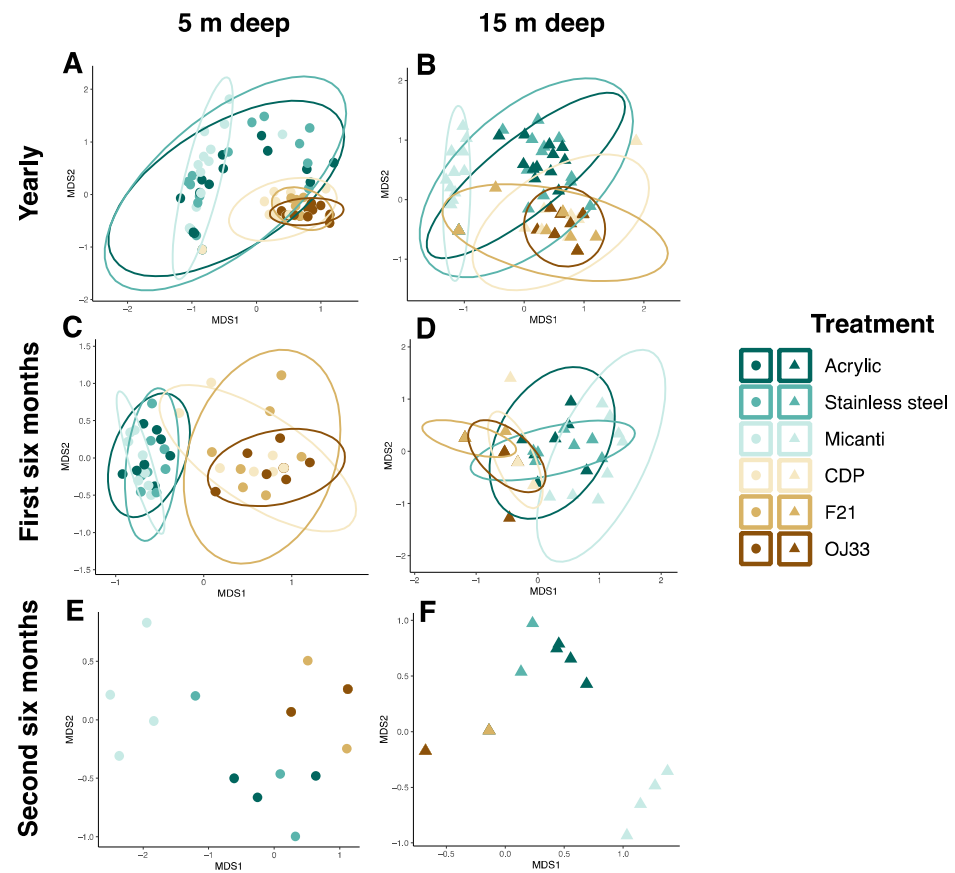


Figure 7. Compositional similarity of the different treatments, that include traditional materials, “eco-friendly”, and not eco-friendly AF strategies. Non-metric multidimensional scaling (NMDS) ordination plots based on abundance data using Bray–Curtis distances at two depths: 5 m deep (A) during 12 months of exposure (stress = 0.139), (C) first (stress = 0.110) and (E) second 6 months of exposure (stress = 0.044), and 15 m (B) during 12 months of exposure (stress = 0.121) and (D) first (stress = 0.140) and (F) second 6 months of exposure (stress = 0.038). The shape represents the different depths (circles for 5 m, triangles for 15 m), surrounded by the ellipse of the 95% confidence interval.

We also found significant differences for richness ($p = 0.004$) and diversity ($p < 0.0001$) between the treatments at 5 m deep (Figure 8A,B). Diversity divided into two groups: acrylic-stainless steel-Micanti and CDP-AF21-OJ33. For richness, it was impossible to separate treatments into groups through post-hoc tests. At 15 m, we found significant differences for richness ($p < 0.0001$) and diversity ($p = 0.001$) between the traditional maritime industry materials and AF coatings (Figure 8C,D). Richness divided into two groups: acrylic-stainless steel-Micanti and CDP-AF21-OJ33. For diversity, it was also impossible to separate treatments into groups through post-hoc tests.

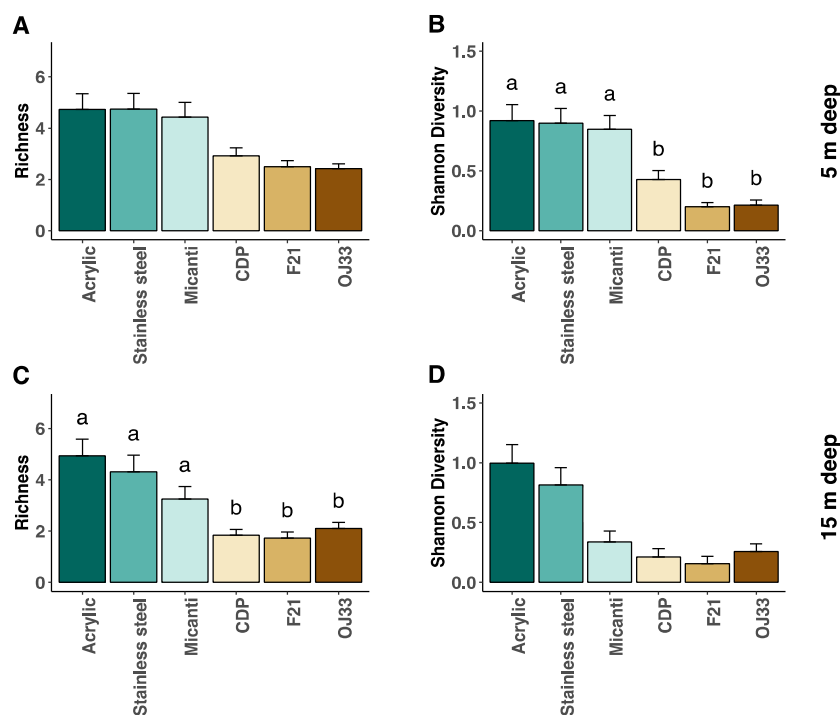


Figure 8. Mean richness (A,C) and Shannon diversity index (B,D) between treatments (mean + SE) at two depths (5 and 15 m). Letters a and b above SE bars indicate significant differences (among treatments from the Dunn's test with an experiment-wise error rate of 0.05).

4. Discussion

In this study, the dominant species and composition of the biofouling community succession were similar to previous studies conducted in central Chile [32,33]. Biofilms and *Obelia geniculata* were the first colonizers, and as succession progressed, substrata were dominated primarily by *Austromegabalanus psittacus* and *Pyura chilensis*. Unlike previous studies, the large sea urchin *Tetrapygus niger* happened to be recruited in large numbers on our experimental plates over the course of the experiment (Supplementary Materials Figure S2). As a result, we glimpsed the potential effect of sea urchin grazing as a biological control of biofouling biomass. Here, we first discuss the experimental results comparing materials and coatings, for which the experiment was designed, and then we consider the preliminary assessment of sea urchin grazing.

Our study contributes to the much-needed comparison between “eco-friendly” and not eco-friendly AF treatments over extended periods in situ. We showed that biofouling cover and biomass increased at similar rates over time among all untreated materials, including the skin-like AF. The two traditional copper-based and the slow-release, “eco-friendly”, AF paints showed similarly low biofouling biomass and richness, demonstrating their efficacy after 12 months in the field and at different depths. The vast majority of readily available AF paints use copper and zinc in the copper oxide and zinc oxide forms as biocides [57]. Studies conducted in diverse marine ecosystems have demonstrated the efficacy of AF against the local flora and fauna [32–34] as well as the short-term AF effect in culture systems [16,32,33,57]. Still, its efficacy in open water and over long periods (years) is understudied, as is the efficacy of more eco-friendly compounds. A recent study compared eco-friendly strategies with copper-based, not eco-friendly, AF coatings in natural environments in the Baltic Sea over one year [58], showing that eco-friendly silicone foul release coatings (FRCs) perform equally well or significantly better than copper coatings. Our study takes this research a step further by comparing the long-term efficacy of “eco-friendly” and not eco-friendly AF treatments in highly wave-exposed environments. It has been suggested that contrasting color differences may impact the

establishment of a biofouling communities, at least in short-term tests of AF coatings. The study [59] showed that fouling species exhibit significantly higher settlement by *Ulva* spp. and spirorbis tube worms on black plastic surfaces compared to white plastic surfaces when exposed at shallow (ca. 40 cm) depths in comparatively short (14 days) experimental trials. The mechanisms producing such differences are unclear and the authors do not offer an explanation, but they may be related to differences in solar radiative heat gains or rugosity between black and white plates. Our study compared three coatings with different colors: CDP (red), OJ33 (red), and F21 (blue) in a highly wave-exposed environment. We did not observe differences in cover or biomass at either depth after a few weeks exposure. Together with previous studies with different materials [32,33], color does not seem to play any significant role in biofouling establishment and growth, at least not after few weeks and at depths beyond few centimeters.

As our results showed, after sea urchin removal, the biomass and cover of the biofouling community resets in the acrylic, stainless steel, and Micanti treatments. Previous studies on the grazing effect on biofouling communities included herbivores such as mollusks [24,29,60], echinoderms [24,26,27,29,31], crustaceans [27,30], and some fish species [29]. Some studies showed that grazing can reduce the biofouling biomass by about 70% and the cover by about 80% [23,24]. Other studies showed that sea urchins significantly reduced the weight of fouling on shellfish aquaculture structures by about 74% [26], and by about 50% independent of biological control organism density [27]. None of these studies evaluated different AF paints, and therefore our study contributes to this body of research, although that was not its original objective. Our study showed an increase in biomass accumulation rate at 5 and 15 m after sea urchin removal in traditional materials (55% and 17%, respectively) and “eco-friendly” and copper-based, not eco-friendly, AF coatings (6% and 3%, respectively). Although biocontrol approaches such as grazing are eco-friendly, our results showed that acrylic, stainless steel, and Micanti treatments require alternative risk mitigation strategies like AF coatings with slow-release technology to reduce biomass cover on artificial structures.

The mean biofouling biomass accumulation (g/day/100 cm²) was affected by exposure time, treatment, depth, and the interaction between exposure time and treatment. Previous research in open systems showed also that exposure time [45–47,61], depth [32,33,61,62], and substrate [32–34] affect the biofouling community assemblage. In our experiment, the biomass accumulation means were different during early versus late succession, and during the 6 month experiment with and without sea urchins. This shows the role grazing plays in controlling biofouling biomass; however, grazing does not eliminate the biofouling problem and must be combined with surface modification strategies that prevent larval settlement.

Depth also affects biofouling biomass, probably due to changes in hydrodynamics, drag and lift forces, as well as tidal and wave regimes that influence the larval and nutrient supplies [62,63]. We found that at 5 m, the biofouling community gained higher biomass than communities at 15 m. This result could also be explained by differences in the oxygen availability [64] at both depths as the deepest frames were beneath the oxycline. Similar differences in biomass and cover by depth were previously described in the same environment [33], suggesting a persistent pattern.

Regarding the treatments, the main sessile biofouling species were *Austromegabalanus psittacus*, *Obelia geniculata*, and *Pyura chilensis* on traditional maritime industry materials (i.e., acrylic and stainless steel) and AF coatings. These species were previously reported for the same area [32,33]. In our experiment, we show that the CDP, AF21, and OJ33 AF coatings inhibit the growth of large organisms such as *Austromegabalanus psittacus* and *Pyura chilensis* and reduce the coverage of the hydrozoan *Obelia geniculata* after one year of exposure. Given the low biomass and cover values for the CDP, AF21, and OJ33 treatments after one year of exposure, we expected diversity to be lower than the other treatments (acrylic, stainless steel, and Micanti) as our result indicated. Additionally, we expected communities between these three treatments to be relatively similar. In contrast, we expected that acrylic would present greater richness, diversity, and dispersion in the

similarity of their communities since acrylic is a widely used material for evaluating composition and succession in benthic systems [32,33,45–47].

Previous studies showed that the OJ33 AF coating prevents any colonization by macrofoulers for more than 7 months under high energy environmental conditions [32]. The CDP AF coating serves as a non-settlement control for multiple-choice larval settlement experiments [65]. However, the present study is the first report for AF21 coating, a paint brand widely used in Chile and throughout the world. Furthermore, we showed that Micanti—an “eco-friendly” AF coating—favors *Pyura chilensis* growth, despite the fact that Micanti AF is advertised as suitable for all circumstances worldwide (i.e., moored or sailing). Our results showed that for moored conditions, this “eco-friendly” strategy is not ideal because it favors the biomass increase of local biofouling communities under moderate waves and currents in central zone conditions. More studies are required to prove its efficacy in sailing conditions.

5. Conclusions

Our results indicate that traditional maritime industry materials and a skin-like “eco-friendly” coating can accumulate biofouling biomass and cover over time at similar rates. The two copper-based, AF paints and the slow-release, “eco-friendly” copper-based paint all showed similar efficacy in controlling biofouling biomass and reduction of biofouling community richness and diversity, which did not decline with depth. Although the slow-release, “eco-friendly” technologies are not completely innocuous to the environment, we recommend this approach over the traditional copper paints, which are both more environmentally aggressive and the most widely used in aquaculture and shipping industries today. However, further research is needed to test whether their environmental impact is significantly lower in the long-term than traditional AF paints, and therefore the search for non-toxic coatings must continue. The mechanical action of skin-like coating did not reduce biofouling and is not recommended in this environment. Our results also suggest that the inclusion of biological control by sea urchins, even in suspended structures, holds potential and should be further investigated.

Supplementary Materials: The following supporting information can be downloaded at: <https://www.mdpi.com/article/10.3390/jmse11010217/s1>. Figure S1. Moorings design and plate location. Figure S2. Urchin recruitment from 1997 to 2019 in the study site. Figure S3. Mean biofouling biomass accumulation rates (g/day/100 cm² ± SE) in the 100 cm² steel and stainless-steel plates recorded during 15 months at the two depths of deployment. Table S1. Description of material and coating characteristics. Table S2. Three main fouling organisms and annual photos. Table S3. (a) Maximum cover percentage (%) value of biofouling species by treatments reached during the experiment. (b) Maximum cover percentage value of oxide by treatments reached at any time of exposure during the experiment. Table S4. a priori contrasts. Table S5. (1,2) Biofouling mean cover percentage between acrylic, stainless steel, and Micanti treatments at 5 and 15 m analyses using repeated measures analysis of variance and checking for sphericity assumption with the Mauchly criteria. (3) Biofouling mean cover percentage by treatment at 5 and 15 m deep after sea urchin removal, using two-way ANOVA. Table S6. Permutational analysis of variance (PERMANOVA) and a posteriori tests using false discovery rate (FDR) correction. Table S7 Richness and diversity analyses.

Author Contributions: Conceptualization, S.A.N., N.O., M.P., M.F. and G.R.F.; methodology, S.A.N., N.O., M.P. and A.E.G.; formal analysis, C.A.-B., N.O., S.A.N. and A.E.G.; data curation, M.P., N.O. and A.E.G.; original draft preparation, C.A.-B., S.A.N. and M.F.; review and editing, C.A.-B., S.A.N. and M.F. All authors have read and agreed to the published version of the manuscript.

Funding: This study was possible thanks to the financial support of the Marine Energy Research and Innovation Center, MERIC, an applied research center funded by the Ministry of Energy and the Production Development Corporation, project CORFO 14CEI2–28228. Additional funding was provided by FONDECYT, grant #1200636 and ANID—Millennium Science Initiative Program—NCN19_05 and COPAS COASTAL ANID FB210021to S.A.N.

Institutional Review Board Statement: Not applicable.

Informed Consent Statement: Not applicable.

Data Availability Statement: Not applicable.

Acknowledgments: We thank all the Coastal Marine Research Station (ECIM) staff at the Pontificia Universidad Católica de Chile and the associated researchers who, in one way or another, helped with this work.

Conflicts of Interest: The authors declare no conflict of interest.

References

1. Callow, J.A.; Callow, M.E. Trends in the Development of Environmentally Friendly Fouling-Resistant Marine Coatings. *Nat. Commun.* **2011**, *2*, 244. [[CrossRef](#)] [[PubMed](#)]
2. Wahl, M. Marine Epibiosis. I. Fouling and Antifouling: Some Basic Aspects. *Mar. Ecol. Prog. Ser.* **1989**, *58*, 175–189. [[CrossRef](#)]
3. Berlow, E.L.; Navarrete, S.A. Spatial and Temporal Variation in Rocky Intertidal Community Organization: Lessons from Repeating Field Experiments. *J. Exp. Mar. Biol. Ecol.* **1997**, *214*, 195–229. [[CrossRef](#)]
4. Paine, R.T. Food Webs: Linkage, Interaction Strength and Community Infrastructure. *J. Anim. Ecol.* **1980**, *49*, 666. [[CrossRef](#)]
5. Yebra, D.M.; Kiil, S.; Dam-Johansen, K. Antifouling Technology—Past, Present and Future Steps towards Efficient and Environmentally Friendly Antifouling Coatings. *Prog. Org. Coat.* **2004**, *50*, 75–104. [[CrossRef](#)]
6. Dafforn, K.A.; Lewis, J.A.; Johnston, E.L. Antifouling Strategies: History and Regulation, Ecological Impacts and Mitigation. *Mar. Pollut. Bull.* **2011**, *62*, 453–465. [[CrossRef](#)]
7. von Ammon, U.; Wood, S.A.; Laroche, O.; Zaiko, A.; Tait, L.; Lavery, S.; Inglis, G.; Pochon, X. The Impact of Artificial Surfaces on Marine Bacterial and Eukaryotic Biofouling Assemblages: A High-Throughput Sequencing Analysis. *Mar. Environ. Res.* **2018**, *133*, 57–66. [[CrossRef](#)]
8. Schultz, M.P.; Bendick, J.A.; Holm, E.R.; Hertel, W.M. Economic Impact of Biofouling on a Naval Surface Ship. *Biofouling* **2011**, *27*, 87–98. [[CrossRef](#)]
9. Titah-Benbouzid, H.; Benbouzid, M. Marine Renewable Energy Converters and Biofouling: A Review on Impacts and Prevention. In Proceedings of the 11th European Wave and Tidal Energy Conference (EWTEC 2015), Nantes, France, 15 September 2015.
10. Gule, N.P.; Begum, N.M.; Klumperman, B. Advances in Biofouling Mitigation: A Review. *Crit. Rev. Environ. Sci. Technol.* **2016**, *46*, 535–555. [[CrossRef](#)]
11. Lewis, J.A. Marine Biofouling and Its Prevention on Underwater Surfaces. *Mater. Forum* **1998**, *22*, 41–61.
12. Singh, N.; Turner, A. Leaching of Copper and Zinc from Spent Antifouling Paint Particles. *Environ. Pollut.* **2009**, *157*, 371–376. [[CrossRef](#)] [[PubMed](#)]
13. Salta, M.; Wharton, J.A.; Stoodley, P.; Dennington, S.P.; Goodes, L.R.; Werwinski, S.; Mart, U.; Wood, R.J.K.; Stokes, K.R. Designing Biomimetic Antifouling Surfaces. *Phil. Trans. R. Soc. A* **2010**, *368*, 4729–4754. [[CrossRef](#)] [[PubMed](#)]
14. Turner, A. Marine Pollution from Antifouling Paint Particles. *Mar. Pollut. Bull.* **2010**, *60*, 159–171. [[CrossRef](#)]
15. Fitrige, I.; Dempster, T.; Guenther, J.; de Nys, R. The Impact and Control of Biofouling in Marine Aquaculture: A Review. *Biofouling* **2012**, *28*, 649–669. [[CrossRef](#)] [[PubMed](#)]
16. Soroldoni, S.; Abreu, F.; Castro, Í.B.; Duarte, F.A.; Pinho, G.L.L. Are Antifouling Paint Particles a Continuous Source of Toxic Chemicals to the Marine Environment? *J. Hazard. Mater.* **2017**, *330*, 76–82. [[CrossRef](#)]
17. Thomas, K.V.; Brooks, S. The Environmental Fate and Effects of Antifouling Paint Biocides. *Biofouling* **2010**, *26*, 73–88. [[CrossRef](#)]
18. Blossom, N. Copper in the Ocean Environment. Deerfield, IL. *Am. Chemet. Corp.* **2007**, 1–8.
19. Kyei, S.K.; Darko, G.; Akaranta, O. Chemistry and Application of Emerging Ecofriendly Antifouling Paints: A Review. *J. Coat. Technol. Res.* **2020**, *17*, 315–332. [[CrossRef](#)]
20. Adeleye, A.S.; Conway, J.R.; Garner, K.; Huang, Y.; Su, Y.; Keller, A.A. Engineered Nanomaterials for Water Treatment and Remediation: Costs, Benefits, and Applicability. *Chem. Eng. J.* **2016**, *286*, 640–662. [[CrossRef](#)]
21. Miller, R.J.; Adeleye, A.S.; Page, H.M.; Kui, L.; Lenihan, H.S.; Keller, A.A. Nano and Traditional Copper and Zinc Antifouling Coatings: Metal Release and Impact on Marine Sessile Invertebrate Communities. *J. Nanopart. Res.* **2020**, *22*, 129. [[CrossRef](#)]
22. Muthukrishnan, T.; Abed, R.M.M.; Dobretsov, S.; Kidd, B.; Finnie, A.A. Long-Term Microfouling on Commercial Biocidal Fouling Control Coatings. *Biofouling* **2014**, *30*, 1155–1164. [[CrossRef](#)]
23. Atalah, J.; Newcombe, E.M.; Zaiko, A. Biocontrol of Fouling Pests: Effect of Diversity, Identity and Density of Control Agents. *Mar. Environ. Res.* **2016**, *115*, 20–27. [[CrossRef](#)]
24. Atalah, J.; Newcombe, E.M.; Hopkins, G.A.; Forrest, B.M. Potential Biocontrol Agents for Biofouling on Artificial Structures. *Biofouling* **2014**, *30*, 999–1010. [[CrossRef](#)] [[PubMed](#)]
25. Marzinelli, E.M.; Underwood, A.J.; Coleman, R.A. Modified Habitats Influence Kelp Epibiota via Direct and Indirect Effects. *PLoS ONE* **2011**, *6*, e21936. [[CrossRef](#)] [[PubMed](#)]
26. Lodeiros, C. The Use of Sea Urchins to Control Fouling during Suspended Culture of Bivalves. *Aquaculture* **2004**, *231*, 293–298. [[CrossRef](#)]
27. Ross, K.A.; Thorpe, J.P.; Brand, A.R. Biological Control of Fouling in Suspended Scallop Cultivation. *Aquaculture* **2004**, *229*, 99–116. [[CrossRef](#)]

28. Sterling, A.M.; Cross, S.F.; Pearce, C.M. Co-Culturing Green Sea Urchins (*Strongylocentrotus droebachiensis*) with Mussels (*Mytilus* Spp.) to Control Biofouling at an Integrated Multi-Trophic Aquaculture Site. *Aquaculture* **2016**, *464*, 253–261. [CrossRef]
29. Davis, A.R.; Benkendorff, K.; Ward, D.W. Responses of Common SE Australian Herbivores to Three Suspected Invasive *Caulerpa* spp. *Mar. Biol.* **2005**, *146*, 859–868. [CrossRef]
30. Dumont, C.P.; Urriago, J.D.; Abarca, A.; Gaymer, C.F.; Thiel, M. The Native Rock Shrimp *Rhynchocinetes typus* as a Biological Control of Fouling in Suspended Scallop Cultures. *Aquaculture* **2009**, *292*, 74–79. [CrossRef]
31. Atalah, J.; Hopkins, G.A.; Forrest, B.M. Augmentative Biocontrol in Natural Marine Habitats: Persistence, Spread and Non-Target Effects of the Sea Urchin *Evechinus chloroticus*. *PLoS ONE* **2013**, *8*, e80365. [CrossRef]
32. Navarrete, S.; Parragué, M.; Osiadacz, N.; Rojas, F.; Bonicelli, J.; Fernandez, M.; Arboleda-Baena, C.; Baldanzi, S. Susceptibility of Different Materials and Antifouling Coating to Macrofouling Organisms in a High Wave-Energy Environment. *J. Ocean. Technol.* **2020**, *15*, 72–91.
33. Navarrete, S.A.; Parragué, M.; Osiadacz, N.; Rojas, F.; Bonicelli, J.; Fernández, M.; Arboleda-Baena, C.; Perez-Matus, A.; Finke, R. Abundance, Composition and Succession of Sessile Subtidal Assemblages in High Wave-Energy Environments of Central Chile: Temporal and Depth Variation. *J. Exp. Mar. Biol. Ecol.* **2019**, *512*, 51–62. [CrossRef]
34. Want, A.; Bell, M.C.; Harris, R.E.; Hull, M.Q.; Long, C.R.; Porter, J.S. Sea-Trial Verification of a Novel System for Monitoring Biofouling and Testing Anti-Fouling Coatings in Highly Energetic Environments Targeted by the Marine Renewable Energy Industry. *Biofouling* **2021**, *37*, 433–451. [CrossRef] [PubMed]
35. Want, A.; Crawford, R.; Kakkonen, J.; Kiddie, G.; Miller, S.; Harris, R.E.; Porter, J.S. Biodiversity Characterisation and Hydrodynamic Consequences of Marine Fouling Communities on Marine Renewable Energy Infrastructure in the Orkney Islands Archipelago, Scotland, UK. *Biofouling* **2017**, *33*, 567–579. [CrossRef] [PubMed]
36. Narváez, D.A.; Poulin, E.; Leiva, G.; Hernández, E.; Castilla, J.C.; Navarrete, S.A. Seasonal and Spatial Variation of Nearshore Hydrographic Conditions in Central Chile. *Cont. Shelf Res.* **2004**, *24*, 279–292. [CrossRef]
37. Tapia, F.J.; Navarrete, S.A.; Castillo, M.; Menge, B.A.; Castilla, J.C.; Largier, J.; Wieters, E.A.; Broitman, B.L.; Barth, J.A. Thermal Indices of Upwelling Effects on Inner-Shelf Habitats. *Prog. Oceanogr.* **2009**, *83*, 278–287. [CrossRef]
38. Wieters, E.; Kaplan, D.; Navarrete, S.; Sotomayor, A.; Largier, J.; Nielsen, K.; Véliz, F. Alongshore and Temporal Variability in Chlorophyll a Concentration in Chilean Nearshore Waters. *Mar. Ecol. Prog. Ser.* **2003**, *249*, 93–105. [CrossRef]
39. Bonicelli, J.; Moffat, C.; Navarrete, S.A.; Largier, J.L.; Tapia, F.J. Spatial Differences in Thermal Structure and Variability within a Small Bay: Interplay of Diurnal Winds and Tides. *Cont. Shelf Res.* **2014**, *88*, 72–80. [CrossRef]
40. Bonicelli, J.; Tapia, F.J.; Navarrete, S.A. Wind-Driven Diurnal Temperature Variability across a Small Bay and the Spatial Pattern of Intertidal Barnacle Settlement. *J. Exp. Mar. Biol. Ecol.* **2014**, *461*, 350–356. [CrossRef]
41. Kaplan, D.M.; Largier, J.L.; Navarrete, S.; Guíñez, R.; Castilla, J.C. Large Diurnal Temperature Fluctuations in the Nearshore Water Column. *Estuar. Coast. Shelf Sci.* **2003**, *57*, 385–398. [CrossRef]
42. Lagos, N.; Navarrete, S.; Véliz, F.; Masuero, A.; Castilla, J. Meso-Scale Spatial Variation in Settlement and Recruitment of Intertidal Barnacles along the Coast of Central Chile. *Mar. Ecol. Prog. Ser.* **2005**, *290*, 165–178. [CrossRef]
43. Navarrete, S.; Largier, J.; Vera, G.; Tapia, F.; Parragué, M.; Ramos, E.; Shinen, J.; Stuardo, C.; Wieters, E. Tumbling under the Surf: Wave-Modulated Settlement of Intertidal Mussels and the Continuous Settlement-Relocation Model. *Mar. Ecol. Prog. Ser.* **2015**, *520*, 101–121. [CrossRef]
44. Piñones, A.; Valle-Levinson, A.; Narváez, D.A.; Vargas, C.A.; Navarrete, S.A.; Yuras, G.; Castilla, J.C. Wind-Induced Diurnal Variability in River Plume Motion. *Estuar. Coast. Shelf Sci.* **2005**, *65*, 513–525. [CrossRef]
45. Cifuentes, M.; Krueger, I.; Dumont, C.P.; Lenz, M.; Thiel, M. Does Primary Colonization or Community Structure Determine the Succession of Fouling Communities? *J. Exp. Mar. Biol. Ecol.* **2010**, *395*, 10–20. [CrossRef]
46. Cifuentes, M.; Kamlah, C.; Thiel, M.; Lenz, M.; Wahl, M. Effects of Temporal Variability of Disturbance on the Succession in Marine Fouling Communities in Northern-Central Chile. *J. Exp. Mar. Biol. Ecol.* **2007**, *352*, 280–294. [CrossRef]
47. Valdivia, N.; Heidemann, A.; Thiel, M.; Molis, M.; Wahl, M. Effects of Disturbance on the Diversity of Hard-Bottom Macrobenthic Communities on the Coast of Chile. *Mar. Ecol. Prog. Ser.* **2005**, *299*, 45–54. [CrossRef]
48. Kuehl, R.O. *Design of Experiments: Statistical Principles of Research Design and Analysis*, 2nd ed.; Duxbury/Thomson Learning: Pacific Grove, CA, USA, 2000.
49. Abelson, R.P.; Prentice, D.A. Contrast Tests of Interaction Hypothesis. *Psychol. Methods* **1997**, *2*, 315. [CrossRef]
50. Escobar, J.; Navarrete, S. Risk Recognition and Variability in Escape Responses among Intertidal Molluscan Grazers to the Sun Star *Heliaster helianthus*. *Mar. Ecol. Prog. Ser.* **2011**, *421*, 151–161. [CrossRef]
51. Racine, J.S. RStudio: A Platform-Independent IDE for R and Sweave. 2012. Available online: <https://posit.co> (accessed on 1 August 2022).
52. Core Team, C. R: A Language and Environment for Statistical Computing. 2013. Available online: <https://www.r-project.org> (accessed on 1 August 2022).
53. Anderson, M.J.; Walsh, D.C.I. PERMANOVA, ANOSIM, and the Mantel Test in the Face of Heterogeneous Dispersions: What Null Hypothesis Are You Testing? *Ecol. Monogr.* **2013**, *83*, 557–574. [CrossRef]
54. Benjamini, Y.; Hochberg, Y. Controlling the False Discovery Rate: A Practical and Powerful Approach to Multiple Testing. *J. R. Stat. Soc. Ser. B Methodol.* **1995**, *57*, 289–300. [CrossRef]

55. Oksanen, J.; Blanchet, F.G.; Friendly, M.; Kindt, R.; Legendre, P.; McGlinn, D.; Minchin, P.; O'Hara, R.; Simpson, G.; Solymos, P. Vegan: Community Ecology Package. R Package Version 2.5-7. 2020. 2021. Available online: <https://cran.r-project.org/web/packages/vegan/vegan.pdf> (accessed on 1 September 2022).
56. Costerton, W.; Lewandowski, Z. Microbial Biofilms. *Annu. Rev. Microbiol.* **1995**, *49*, 711–745. [[CrossRef](#)] [[PubMed](#)]
57. Instituto de Fomento Pesquero, IFOP. *Evaluación de Los Efectos de Las Pinturas Anti-Incrustantes en Las Comunidades Bentónicas Del Medio Marino*; Instituto De Fomento Pesquero(IFOP): Valparaíso, Chile, 2017; p. 362.
58. Lagerström, M.; Wrangé, A.-L.; Oliveira, D.R.; Granhag, L.; Larsson, A.L.; Ytreberg, E. Are Silicone Foul-Release Coatings a Viable and Environmentally Sustainable Alternative to Biocidal Antifouling Coatings in the Baltic Sea Region? *Mar. Pollut. Bull.* **2022**, *184*, 114102. [[CrossRef](#)]
59. Swain, G.; Herpe, S.; Ralston, E.; Tribou, M. Short-Term Testing of Antifouling Surfaces: The Importance of Colour. *Biofouling* **2006**, *22*, 425–429. [[CrossRef](#)]
60. Arboleda-Baena, C.; Pareja, C.B.; Pla, I.; Logares, R.; De la Iglesia, R.; Navarrete, S.A. Hidden Interactions in the Intertidal Rocky Shore: Variation in Pedal Mucus Microbiota among Marine Grazers That Feed on Epilithic Biofilm Communities. *PeerJ* **2022**, *10*, e13642. [[CrossRef](#)] [[PubMed](#)]
61. Bram, J.B.; Page, H.M.; Dugan, J.E. Spatial and Temporal Variability in Early Successional Patterns of an Invertebrate Assemblage at an Offshore Oil Platform. *J. Exp. Mar. Biol. Ecol.* **2005**, *317*, 223–237. [[CrossRef](#)]
62. Glasby, T.; Connell, S. Orientation and Position of Substrata Have Large Effects on Epibiotic Assemblages. *Mar. Ecol. Prog. Ser.* **2001**, *214*, 127–135. [[CrossRef](#)]
63. Denny, M.W. Life in the Maelstrom: The Biomechanics of Wave-Swept Rocky Shores. *Trends Ecol. Evol.* **1987**, *2*, 61–66. [[CrossRef](#)] [[PubMed](#)]
64. Thiel, M.; Macaya, E.; Acuña, E.; Arntz, W.; Bastias, H.; Brokordt, K.; Camus, P.; Castilla, J.; Castro, L.; Cortés, M.; et al. The Humboldt Current System of Northern and Central Chile: Oceanographic Processes, Ecological Interactions And Socioeconomic Feedback. In *Oceanography and Marine Biology: An Annual Review*; Gibson, R., Atkinson, R., Gordon, J., Eds.; CRC Press: Boca Raton, FL, USA, 2007; Volume 45, pp. 195–344, ISBN 978-1-4200-5093-6. [[CrossRef](#)]
65. Baldanzi, S.; Vargas, I.T.; Armijo, F.; Fernández, M.; Navarrete, S.A. Experimental Assessment of a Conducting Polymer (PEDOT) and Microbial Biofilms as Deterrents and Facilitators of Macro-Biofouling: Larval Settlement of the Barnacle *Notobalanus Flosculus* (Darwin, 1854) from Central Chile. *J. Mar. Sci. Eng.* **2021**, *9*, 82. [[CrossRef](#)]

Disclaimer/Publisher's Note: The statements, opinions and data contained in all publications are solely those of the individual author(s) and contributor(s) and not of MDPI and/or the editor(s). MDPI and/or the editor(s) disclaim responsibility for any injury to people or property resulting from any ideas, methods, instructions or products referred to in the content.